

Many-body localization transition in large quantum spin chains: The mobility edge

Titas Chanda,^{1,*} Piotr Sierant,^{1,†} and Jakub Zakrzewski^{1,2,‡}

¹*Instytut Fizyki Teoretycznej, Uniwersytet Jagielloński, Łojasiewicza 11, 30-348 Kraków, Poland*

²*Mark Kac Complex Systems Research Center, Uniwersytet Jagielloński, Kraków, Poland.*

(Dated: October 13, 2020)

Thermalization of random-field Heisenberg spin chain is probed by time evolution of density correlation functions. Studying the impacts of average energies of initial product states on dynamics of the system, we provide arguments in favor of the existence of a mobility edge in the large system-size limit.

Introduction.— Many-body localization (MBL) [1, 2] is a robust mechanism that prevents reaching of thermal equilibrium by quantum many-body systems [3–5]. The phenomenon, originating from an interplay of interactions and disorder [6–8], has been studied numerically in various models: spin chains [9–12] that map onto spinless fermionic chains, spinful fermions [13–16] or bosons [17–19]. Despite those efforts, a complete understanding of the transition between ergodic and MBL phases is still lacking. While the recent works [20–24] suggest a Kosterlitz-Thouless scaling at the MBL transition, it became clear that the exact diagonalization studies are subject to strong finite size effects [25–27] that prevent one from reaching unambiguous conclusions about the thermodynamic limit [28, 29].

Alternatively, time evolution of large [30] (or even infinite [31]) disordered many-body systems can be simulated with tensor network algorithms. Reaching large time scales, necessary to assess thermalization properties [32] is challenging especially in the vicinity of transition to ergodic phase. Nevertheless, such an approach allows to obtain estimates for critical disorder strength for large system sizes [30, 32], in quasiperiodic systems [33], or even beyond one spatial dimension [34, 35]. An advantage of such an approach is that it directly mimics experimental observations of MBL [36–43].

Typically, the transition between ergodic and MBL phases is induced by tuning the disorder strength. Then the natural extension is – can one envision a different control parameter? In this work, we consider energy as such a parameter. This immediately translates to a problem of the existence of *many-body mobility edges*, i.e., energies that separate localized and extended states [2]. The many-body mobility edges observed in early exact diagonalization studies of small systems [12, 44, 45] were argued to be indistinguishable from finite-size effects in [46]. The argument of [46] is that local fluctuations in a system with a putative many-body mobility edge can serve as mobile bubbles inducing a global delocalization and hence no many-body mobility edge can exist. The existence of mobility edges is one of the fundamen-

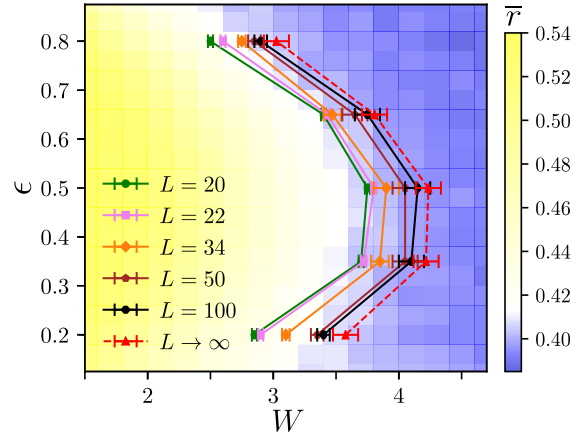


FIG. 1. Phase diagram of random-field Heisenberg spin chain, disorder strength W on horizontal axis, rescaled energy ϵ on vertical axis. Background shows color-coded value of average gap ratio \bar{r} for system size $L = 16$. Solid lines show the position of boundary between ergodic and MBL phases obtained in study of decay of density correlations in systems of size $L = 20, 22, 26, 34, 50, 100$, dashed line shows results of extrapolation of the results to $L \rightarrow \infty$.

tal problems of MBL, it leads to questions about phenomenology of systems with many-body mobility edge (since the description in terms of local integrals of motion [47–53] does not apply in such a scenario), or to the anomalous dynamics for a non-stationary initial state due to energy fluctuations [54, 55].

The aim of our work is to study many-body mobility edges at much larger system sizes than those available to exact diagonalization in an attempt to verify conclusions of [46]. To that end, we employ Chebyshev polynomial expansion of the evolution operator [56–58] and the time-dependent variational principle (TDVP) applied to matrix product states (MPS) [59–62] to simulate time dynamics of random-field Heisenberg spin chain. Our approach is, in spirit, similar to that of [63] and [64] (and used for bosons in [65]). However, instead of considering an injection of controllable amount of energy into ground state of the system, we consider time evolution of initial product states with specified average energies, exactly similar to what was done recently in spin quantum simulator [66]. Probing time decay of density correlation functions allows us to estimate the critical disorder strength

* titas.chanda@uj.edu.pl

† piotr.sierant@uj.edu.pl

‡ jakub.zakrzewski@uj.edu.pl

as a function of energy of the initial state. Studying systems of size up to $L = 100$, we perform a finite size scaling of our results which provides arguments in favor of existence of mobility edge even in large systems.

The model and methods.— We consider 1D random-field Heisenberg (XXZ) spin chain with the Hamiltonian given by

$$H = J \sum_{i=1}^{L-1} (S_i^x S_{i+1}^x + S_i^y S_{i+1}^y + S_i^z S_{i+1}^z) + \sum_{i=1}^L h_i S_i^z, \quad (1)$$

where S_i^α , $\alpha = x, y, z$, are spin-1/2 matrices, $J = 1$ is fixed to be the unit of energy, and $h_i \in [-W, W]$ are independent, uniformly distributed random variables. In this work, we consider open boundary conditions in the Hamiltonian (1). The random-field Heisenberg spin chain has been widely studied in the MBL context [12, 31, 67–73], which has made it the *de facto* standard model of MBL studies.

The transition between ergodic and MBL phases is reflected in change of statistical properties of energy levels of the system. A common approach is to consider the gap ratio $r_i = \frac{\min\{E_{i+2}-E_{i+1}, E_{i+1}-E_i\}}{\max\{E_{i+2}-E_{i+1}, E_{i+1}-E_i\}}$, where E_i are the energy eigenvalues of the system. Averaging the gap ratio over part of the spectrum of the system and over disorder realizations, one obtains an average gap ratio \bar{r} , which differentiates between level statistics of ergodic system [10, 74], well described by Gaussian orthogonal ensemble of random matrices, for which $\bar{r} \approx 0.53$ and between Poissonian statistics of eigenvalues in MBL phase (for which $\bar{r} \approx 0.39$). The later arises due to emergent integrability resulting from the presence of local integrals of motion [47–53].

To reveal the dependence of ergodic-MBL transition on energy, the gap ratios r_i are averaged over only a certain number of eigenvalues with energies close to a rescaled energy $\epsilon = (E - E_{\min}) / (E_{\max} - E_{\min})$, where E_{\min} (E_{\max}) is the energy of the ground (highest excited) state. Such a calculation of average gap ratio (supported with results for other probes of localization) for random-field Heisenberg spin chain reveals that the ergodic region has shape of a characteristic lobe on the phase diagram in variables of the rescaled energy ϵ and disorder strength W [12]. The average gap ratio, obtained in exact diagonalization of random field Heisenberg spin chain of size $L = 16$, is plotted as a function of ϵ and W in the background of Fig. 1.

To probe the transition between ergodic and MBL phases with time evolution, we propose the following protocol. We consider an initial state $|\psi\rangle = |\sigma_1, \dots, \sigma_L\rangle$, where $\sigma_i = \uparrow, \downarrow$ are chosen randomly with constraint that the average rescaled energy $\epsilon_\psi = (\langle\psi|H|\psi\rangle - E_{\min}) / (E_{\max} - E_{\min})$ of this state lies within the range $[\epsilon - \delta\epsilon, \epsilon + \delta\epsilon]$ corresponding to a given rescaled energy ϵ , where $\delta\epsilon$ is a small tolerance (we take $\delta\epsilon = 0.01$). To calculate ϵ_ψ for $L \leq 26$ we find E_{\max}, E_{\min} with the standard Lanczos algorithm [75]. For larger system sizes, E_{\min} and E_{\max} are calculated using density matrix renor-

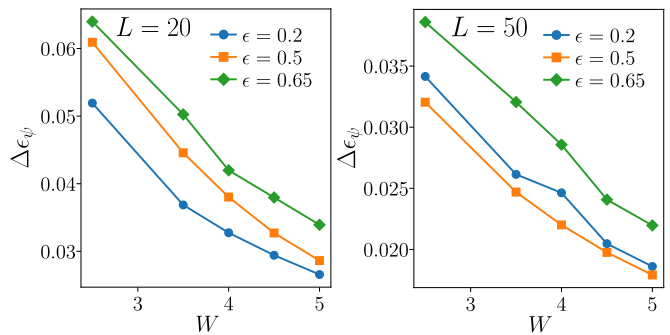


FIG. 2. Disorder averaged standard deviation $\Delta\epsilon_\psi$ of rescaled energy of the initial states as a function of disorder strength W for three exemplary rescaled energies ϵ . Left: system size $L = 20$, Right: system size: $L = 50$.

malization group (DMRG) algorithm [76–80] (see [81] for details).

Subsequently, we calculate time evolved state $|\psi(t)\rangle = e^{-iHt}|\psi\rangle$ with the standard Chebyshev expansion of the evolution operator [58] for $L \leq 26$. For larger system sizes, we use the recently developed TDVP algorithm [59–62]. Technically, we follow [32, 82] and employ a hybrid of two-site and one-site versions of TDVP [62, 83] (see [81] for details).

Our quantity of interest is the density correlation function

$$C(t) = D \sum_{i=1+l_0}^{L-l_0} \langle\psi(t)|S_i^z|\psi(t)\rangle \langle\psi|S_i^z|\psi\rangle, \quad (2)$$

where the constant D assures that $C(0) = 1$ and $l_0 > 0$ diminishes the influence of boundaries (in our calculations, we take $l_0 = 2$). The standard deviation of the rescaled energy

$$\Delta\epsilon_\psi = \left(\langle\psi| ((H - E_{\min}) / (E_{\max} - E_{\min}) - \epsilon_\psi)^2 |\psi\rangle \right)^{1/2} \quad (3)$$

is smaller than 0.1 for disorder strengths that we consider in this work as shown in Fig. 2. Those relatively small fluctuations of energy suggest that the properties of eigenstates at the rescaled energy ϵ can be well probed by time evolution of the state $|\psi\rangle$ and reflected, in particular, by the density correlation function $C(t)$.

Quench dynamics: dependence on disorder strength.— Fig. 3 shows the density correlation functions $C(t)$ obtained for the random-field Heisenberg spin chain of a fixed size $L = 20$, for rescaled energy $\epsilon = 0.5$ of the initial state. The correlation function decreases in time, with some oscillations superimposed [84]. For small disorder strength, e.g. $W = 2.8$ the eigenstate thermalization hypothesis [5, 85] is valid for the system, and in the long time limit the correlation function vanishes $C(t) \xrightarrow{t \rightarrow \infty} 0$ as system loses the memory of the initial state. In contrast, for large disorder strength, e.g., $W = 5$, a non-zero stationary value of the correlation function $C(t) \xrightarrow{t \rightarrow \infty} c_0 > 0$

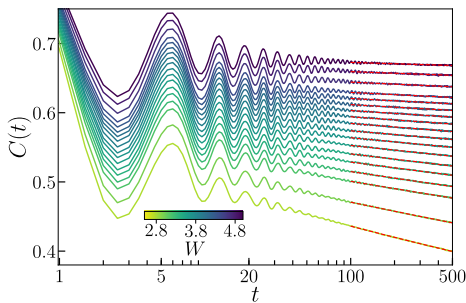


FIG. 3. Quench dynamics in disordered XXZ spin chain. Density correlation function $C(t)$ for system size $L = 20$ and various disorder strengths $W = 2.8, \dots, 5$ (color coded) averaged over 10000 disorder realizations, rescaled energy of the initial state $\epsilon = 0.5$, power-law fits $C(t) \propto t^{-\beta}$ for $t \in [100, 500]$ are denoted by the dashed lines.

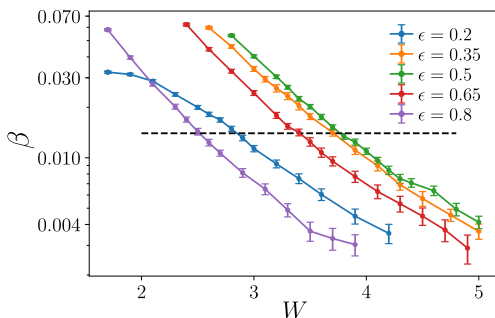


FIG. 4. The exponent β , obtained in fitting the density correlation function $C(t)$ with an algebraic decay $a_0 t^{-\beta}$ in interval $t \in [100, 500]$, is plotted as function of disorder strength W . The errorbars represent the 1σ errors of the fitting obtained from statistical resampling of disorder realizations. The system size is $L = 20$, results for various rescaled energies ϵ of the initial state are shown. The dashed line shows the cut-off exponent $\beta_0 = 0.014$.

is admitted showing that the system is non-ergodic. The first experimental signatures of MBL were obtained in study of time evolution of *imbalance* [36], quantity analogous to the density correlation function – for quantitative comparison of the two quantities see [81].

At large times ($t > 100$), the decay of the correlation function is well described by a power law, $C(t) \propto t^{-\beta}$. Griffiths rare regions are one possible explanation of this behavior [86]. However, it was shown experimentally and numerically that time dynamics in quasiperiodic potentials, where Griffiths regions are necessarily absent, have analogous features [70, 87, 88]. Regardless of the origin of the power law decay of the correlation function, the disorder strength dependence of the exponent β can be used to locate the onset of ergodicity breaking in the system.

The exponent β governing the decay of the density correlation function is shown in Fig. 4(a). Let us first concentrate on the results in the middle of the spectrum ($\epsilon = 0.5$). In the considered interval of disorder strength W , the exponent decreases exponentially with W with a

good approximation $\beta \propto e^{-W/\Omega}$. The large number of disorder realizations (10000) used in calculation of $C(t)$ allows us to see that even at the large disorder strength $W = 5$ the exponent $\beta = 4.1(4) \cdot 10^{-3}$ is non-vanishing. If the power-law decay $C(t) = a_0 t^{-\beta}$ prevailed for $t \rightarrow \infty$, the density correlation function would vanish in the long-time limit and the system would be ergodic. This, however, does not happen for $L = 20$, as after the so-called Heisenberg time t_H discreteness of spectrum manifests itself in saturation of the correlation functions [89–92], so that one would observe $C(t) \xrightarrow{t \rightarrow \infty} c_0 > 0$ for $W = 5$ and $L = 20$. The Heisenberg time t_H increases exponentially with the system size L . This illustrates a difficulty in locating the MBL transition using time dynamics of large systems on time scales of few hundred J^{-1} accessible to tensor network methods (or to current experiments with e.g., ultra-cold atoms): one cannot predict whether a slow decay of correlation functions governed by an exponent $\beta \ll 1$ observed, for example $t \in [100, 500]$, will eventually lead to $C(t) \xrightarrow{t \rightarrow \infty} 0$ or not.

To resolve the difficulties, the work of [30] assumes that the value of the exponent β must be vanishing within error bars to be compatible with saturation of correlation functions in the long time limit. The drawback of this criterion is that the error bar of β depends on the number of disorder realizations used in calculation of the correlation function. Therefore, we introduce a cut-off β_0 : disorder strength $W_C(L)$ for which $\beta = \beta_0$ is regarded as disorder strength for transition to MBL phase at system size L . Exact diagonalization results show that: i) collapse of data for $L \leq 22$ gives a critical disorder strength $W_C \approx 3.7$; ii) the similar values $W_C \approx 3.8$ or $W_C \approx 4.2$ are obtained in asymmetric scaling on the two sides of the transition; iii) the breakdown of the volume-law scaling of entanglement entropy gives an estimate $W_C = 3.75$ at system size $L = 20$ [29]. The obtained results for β at $L = 20$ and $\epsilon = 0.5$ show that the cut-off value $\beta_0 = 0.014$ is consistent with the above estimates for the critical disorder strength obtained from exact diagonalizations, see Fig. 4. The assumed cut-off value β_0 is nearly independent of the target energy and system size (for further details see [81]). Consequently, throughout this work, we use $\beta_0 = 0.014$ as a threshold value which separates ergodic and MBL regimes for all system sizes and energies of the initial state we consider.

The values of β presented in Fig. 4(a) show that the increase of disorder strength W slows down the dynamics more severely for rescaled energies of initial state different than $\epsilon = 0.5$. Notably, the exponent β decreases exponentially with W : $\beta \propto e^{-W/\Omega}$ (where Ω is a constant) in a wide regime of disorder strengths. This resembles the scaling of Thouless time $t_{Th} \propto e^{-W/W_0}$ observed in exact diagonalization data in [25].

Quench dynamics: dependence on system size.– Density correlation function $C(t)$ for larger system sizes are shown for two exemplary pairs of disorder strength W and initial rescaled energy ϵ in Fig. 5. The decay of $C(t)$ at large times is well fitted by an algebraic dependence

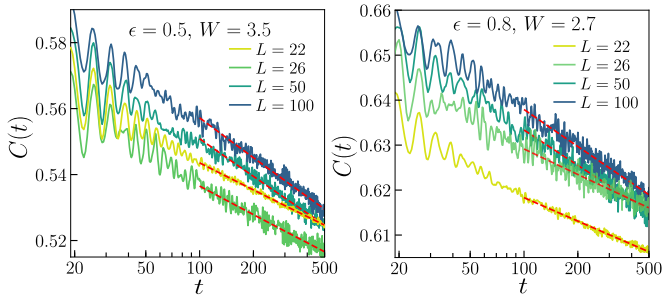


FIG. 5. Time evolution of density correlation function $C(t)$ for rescaled energy of initial state $\epsilon = 0.5$ ($\epsilon = 0.8$) and disorder strength $W = 3.5$ ($W = 2.7$) in panel right (left). The system size L varies from 22 to 100. The dashed lines denote power-law fits $C(t) = a_0 t^{-\beta}$ in the $t \in [100, 500]$ interval.

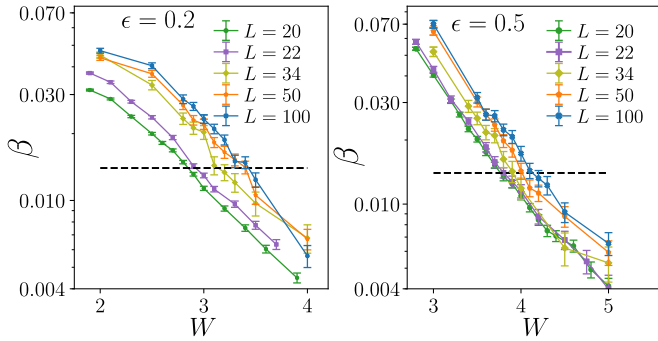


FIG. 6. The exponent β obtained in fitting the density correlation function $C(t)$ with an algebraic decay $a_0 t^{-\beta}$ in interval $t \in [100, 500]$ for the rescaled energy $\epsilon = 0.2$ ($\epsilon = 0.5$) of the initial state shown in the left (right) panel. Data shown for system sizes $L = 20, 22, 34, 50, 100$. The error bars show 1σ errors of β obtained in resampling of disorder realizations. The dashed lines show the cut-off exponent β_0 .

$C(t) \propto t^{-\beta}$. The exponents β obtained in the fitting of power-law decay to $C(t)$ are shown for two exemplary values of the rescaled energy ϵ of the initial states in Fig. 6. For a given disorder strength W , we observe a clear increase of β with increasing system size. Interestingly, the shift is, to a good approximation, uniform for all disorder strengths so that the exponential decrease $\beta \propto e^{-W/\Omega}$ (at sufficiently large W) is observed for all considered system sizes. Let us mention here that we consider 400 realizations of disorder for $L = 34, 50$, and 200 realizations for $L = 100$ for each values of ϵ and W . For small system sizes ($L = 20, 22, 26$) we consider between 10000 and 500 disorder realizations.

We obtain estimates for disorder strength $W_C(L)$ for transition to MBL phase by finding the crossings of $\beta(W)$ curve for given system size L with the $\beta = \beta_0$ line. Results of this procedure are shown in Fig. 7(a). The disorder strength $W_C(L)$ depend, within the estimated error bars, linearly on the inverse of the system size L with clear growth of $W_C(L)$ as the system size increases. On one hand, this trend allows us, by means of a linear fit $W_C(1/L) = A/L + W_C(\infty)$, to extrapolate the results to

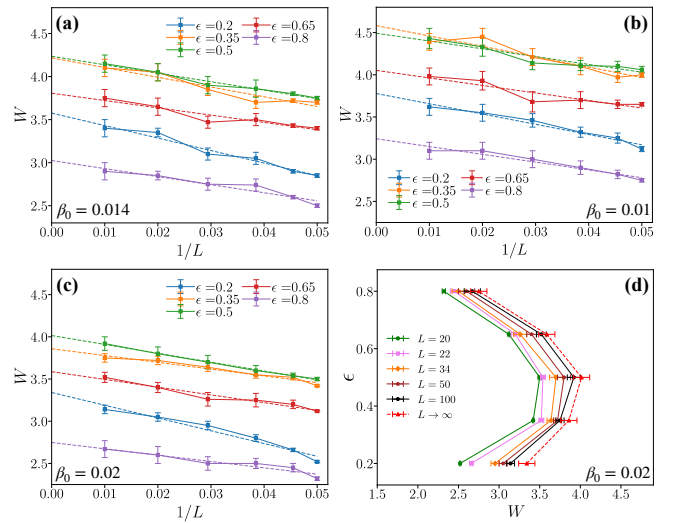


FIG. 7. (a) Disorder strength $W_C(L)$ for which decay of correlation function is governed by power-law with $\beta = \beta_0$ plotted as function of $1/L$ where L is the system size. Results shown for various rescaled energies ϵ of initial state. Available data are fitted with linear functions $W_C(1/L) = A/L + W_C(\infty)$ which allow extrapolation to $L \rightarrow \infty$. (b)-(c) Same as in (a), but with two different choices of cut-off β_0 (0.01 and 0.02 respectively). (d) The shape of the edge between localized and delocalized regions in (ϵ, W) -plane for different system-sizes $L = 20, 20, 34, 50, 100$ obtained with threshold $\beta_0 = 0.02$. Dashed line shows the extrapolation of the results for $L \rightarrow \infty$.

$L \rightarrow \infty$ and to obtain the estimate of critical disorder strength $W_C(\infty)$ for transition to MBL phase.

On the other hand, we observe that the slopes A are similar for all of the considered rescaled energies of the initial state. Thus, the shape of the boundary between ergodic and MBL regimes observed for $L = 20$ does not change considerably when the system size is increased. This is visible in Fig. 1. The points for various system sizes L are precisely the values of $W_C(L)$ obtained from the condition $\beta = \beta_0$. The characteristic shape of the lobe does not change when the system sizes increases from $L = 20$ to $L = 100$ and is preserved even after the extrapolation to $L \rightarrow \infty$. Therefore, there exists a certain range of disorder strengths such that the states for $\epsilon < \epsilon_{ME}^L$ are localized, states for $\epsilon_{ME}^L < \epsilon < \epsilon_{ME}^U$ are extended and states for $\epsilon > \epsilon_{ME}^U$ are again localized. Thus, our results indicate that the system indeed possesses a many-body mobility edge in the thermodynamic limit.

Upto now, the results are reported with the threshold value $\beta_0 = 0.014$. However, the qualitative results and the conclusion about the existence of mobility edge in large systems remain unaltered for different choices of β_0 , which we show in Figs. 7(b) and (c) by considering $\beta_0 = 0.01$ and 0.02 respectively. However, very small choice of β_0 (e.g., 0.01) results in larger error bars, which points towards the difficulty of obtaining the saturation of the correlation function within finite interval of time with

finite number of disorder realizations. Fig. 7(d) shows the shapes of the boundary between MBL and delocalized obtained for $\beta_0 = 0.02$ at different system-sizes, which remain qualitatively same as those for $\beta_0 = 0.014$.

Discussion and outlook.— Chebyshev polynomial expansion of the time evolution operator and the TDVP method applied to MPS allowed us to study the problem of energy dependence of the transition between ergodic and MBL phases in large disordered quantum spin chains. Introducing a cut-off value of exponent β of power-law decay in time of density correlation function, we were able to probe the transition for different rescaled energies of the initial state. For small system-sizes (e.g., $L = 20$), our approach gives results consistent with exact diagonalization. Importantly, our method allows to consider much larger system sizes ($L = 100$) for which it predicts an existence of a mobility edge.

The disorder strength $W_C(L)$ is a lower bound on the transition to MBL phase: the residual decay of density correlations with exponent β_0 is insufficient to restore the uniform density profile for system size $L = 20$, but it is possible that it leads to an eventual decay of correlation function for larger system sizes.

The protocol we considered is, in principle, experimentally realizable. Our results can be verified experimentally if the setup of [66] was scaled to larger system sizes. Many-body mobility edge arises also in disordered Bose-Hubbard models [93]. It can be probed by a quench

protocol analogous to the one considered in this work. Since the bosonic models allow for occupations in each site larger than unity, density wave-like states that are easier to obtain in an experiment with ultra-cold atoms can be used to probe the many-body mobility edge [65, 93]. When this work was close to completion, we have learnt about a recent study [94] where many-body mobility edge with respect to particle numbers were shown to exist in a correlated hopping model of hardcore bosons.

ACKNOWLEDGMENTS

Support of the Polish National Science Centre via grants Unisono 2017/25/Z/ST2/03029 (T.C.) (under QTFLAG Quanterra collaboration), Opus 2015/19/B/ST2/01028 (P.S.), and Opus 2019/35/B/ST2/00034 (J.Z.) is acknowledged. P.S. thanks the Polish National Science Centre for an additional support via Etiuda programme 2018/28/T/ST2/00401 as well as the Foundation for Polish Science (FNP) through scholarship START. The partial support by PL-Grid Infrastructure is also acknowledged. The MPS-based techniques have been implemented using ITensor library v2 (<https://itensor.org>).

-
- [1] I. V. Gornyi, A. D. Mirlin, and D. G. Polyakov, *Phys. Rev. Lett.* **95**, 206603 (2005).
 - [2] D. Basko, I. Aleiner, and B. Altshuler, *Ann. Phys. (NY)* **321**, 1126 (2006).
 - [3] J. M. Deutsch, *Phys. Rev. A* **43**, 2046 (1991).
 - [4] M. Srednicki, *Phys. Rev. E* **50**, 888 (1994).
 - [5] M. Rigol, V. Dunjko, and M. Olshanii, *Nature* **452**, 854 EP (2008).
 - [6] R. Nandkishore and D. A. Huse, *Ann. Rev. Cond. Mat. Phys.* **6**, 15 (2015).
 - [7] F. Alet and N. Laflorencie, *Comptes Rendus Physique* **19**, 498 (2018).
 - [8] D. A. Abanin, E. Altman, I. Bloch, and M. Serbyn, *Rev. Mod. Phys.* **91**, 021001 (2019).
 - [9] L. F. Santos, G. Rigolin, and C. O. Escobar, *Phys. Rev. A* **69**, 042304 (2004).
 - [10] V. Oganesyan and D. A. Huse, *Phys. Rev. B* **75**, 155111 (2007).
 - [11] A. Pal and D. A. Huse, *Phys. Rev. B* **82**, 174411 (2010).
 - [12] D. J. Luitz, N. Laflorencie, and F. Alet, *Phys. Rev. B* **91**, 081103 (2015).
 - [13] R. Mondaini and M. Rigol, *Phys. Rev. A* **92**, 041601 (2015).
 - [14] P. Prelovšek, O. S. Barišić, and M. Žnidarič, *Phys. Rev. B* **94**, 241104 (2016).
 - [15] J. Zakrzewski and D. Delande, *Phys. Rev. B* **98**, 014203 (2018).
 - [16] M. Kozarzewski, P. Prelovšek, and M. Mierzejewski, *Phys. Rev. Lett.* **120**, 246602 (2018).
 - [17] P. Sierant, D. Delande, and J. Zakrzewski, *Phys. Rev. A* **95**, 021601 (2017).
 - [18] T. Orell, A. A. Michailidis, M. Serbyn, and M. Silveri, *Phys. Rev. B* **100**, 134504 (2019).
 - [19] M. Hopjan and F. Heidrich-Meisner, “Many-body localization from a one-particle perspective in the disordered 1d bose-hubbard model,” [arXiv:1912.09443](https://arxiv.org/abs/1912.09443).
 - [20] A. Goremykina, R. Vasseur, and M. Serbyn, *Phys. Rev. Lett.* **122**, 040601 (2019).
 - [21] A. Morningstar and D. A. Huse, *Phys. Rev. B* **99**, 224205 (2019).
 - [22] P. T. Dumitrescu, A. Goremykina, S. A. Parameswaran, M. Serbyn, and R. Vasseur, *Phys. Rev. B* **99**, 094205 (2019).
 - [23] N. Laflorencie, G. Lemarié, and N. Macé, “Chain breaking and Kosterlitz-Thouless scaling at the many-body localization transition,” [arXiv:2004.02861](https://arxiv.org/abs/2004.02861).
 - [24] J. Šuntajs, J. Bonča, T. Prosen, and L. Vidmar, “Ergodicity breaking transition in finite disordered spin chains,” (2020), [arXiv:2004.01719](https://arxiv.org/abs/2004.01719).
 - [25] J. Šuntajs, J. Bonča, T. Prosen, and L. Vidmar, [arXiv:1905.06345](https://arxiv.org/abs/1905.06345).
 - [26] P. Sierant, D. Delande, and J. Zakrzewski, *Phys. Rev. Lett.* **124**, 186601 (2020).
 - [27] D. A. Abanin, J. H. Bardarson, G. D. Tomasi, S. Gopalakrishnan, V. Khemani, S. A. Parameswaran, F. Pollmann, A. C. Potter, M. Serbyn, and R. Vasseur, [arXiv:1911.04501](https://arxiv.org/abs/1911.04501).

- [28] R. K. Panda, A. Scardicchio, M. Schulz, S. R. Taylor, and M. Žnidarič, *EPL (Europhysics Letters)* **128**, 67003 (2020).
- [29] P. Sierant, M. Lewenstein, and J. Zakrzewski, “Polynomially filtered exact diagonalization approach to many-body localization,” [arXiv:2005.09534](https://arxiv.org/abs/2005.09534).
- [30] E. V. H. Doggen, F. Schindler, K. S. Tikhonov, A. D. Mirlin, T. Neupert, D. G. Polyakov, and I. V. Gornyi, *Phys. Rev. B* **98**, 174202 (2018).
- [31] T. Enss, F. Andraschko, and J. Sirker, *Phys. Rev. B* **95**, 045121 (2017).
- [32] T. Chanda, P. Sierant, and J. Zakrzewski, *Phys. Rev. B* **101**, 035148 (2020).
- [33] E. V. H. Doggen and A. D. Mirlin, *Phys. Rev. B* **100**, 104203 (2019).
- [34] C. Hubig and J. I. Cirac, *SciPost Phys.* **6**, 31 (2019).
- [35] E. V. H. Doggen, I. V. Gornyi, A. D. Mirlin, and D. G. Polyakov, “Slow many-body delocalization beyond one dimension,” [arXiv:2002.07635](https://arxiv.org/abs/2002.07635).
- [36] M. Schreiber, S. S. Hodgman, P. Bordia, H. P. Lüschen, M. H. Fischer, R. Vosk, E. Altman, U. Schneider, and I. Bloch, *Science* **349**, 842 (2015).
- [37] P. Bordia, H. Lüschen, U. Schneider, M. Knap, and I. Bloch, *Nature Physics* **13**, 460 EP (2017), article.
- [38] T. Kohlert, S. Scherg, X. Li, H. P. Lüschen, S. Das Sarma, I. Bloch, and M. Aidelsburger, *Phys. Rev. Lett.* **122**, 170403 (2019).
- [39] A. Lukin, M. Rispoli, R. Schittko, M. E. Tai, A. M. Kaufman, S. Choi, V. Khemani, J. Léonard, and M. Greiner, *Science* **364**, 256 (2019).
- [40] M. Rispoli, A. Lukin, R. Schittko, S. Kim, M. E. Tai, J. Léonard, and M. Greiner, *Nature* **573**, 385 (2019).
- [41] J.-y. Choi, S. Hild, J. Zeiher, P. Schauß, A. Rubio-Abadal, T. Yefsah, V. Khemani, D. A. Huse, I. Bloch, and C. Gross, *Science* **352**, 1547 (2016).
- [42] J. Smith, A. Lee, P. Richerme, B. Neyenhuis, P. W. Hess, P. Hauke, M. Heyl, D. A. Huse, and C. Monroe, *Nature Physics* **12**, 907 (2016).
- [43] K. Xu, J.-J. Chen, Y. Zeng, Y.-R. Zhang, C. Song, W. Liu, Q. Guo, P. Zhang, D. Xu, H. Deng, K. Huang, H. Wang, X. Zhu, D. Zheng, and H. Fan, *Phys. Rev. Lett.* **120**, 050507 (2018).
- [44] J. A. Kjäll, J. H. Bardarson, and F. Pollmann, *Phys. Rev. Lett.* **113**, 107204 (2014).
- [45] I. Mondragon-Shem, A. Pal, T. L. Hughes, and C. R. Laumann, *Phys. Rev. B* **92**, 064203 (2015).
- [46] W. De Roeck, F. Huveneers, M. Müller, and M. Schiulaz, *Phys. Rev. B* **93**, 014203 (2016).
- [47] M. Serbyn, Z. Papić, and D. A. Abanin, *Phys. Rev. Lett.* **111**, 127201 (2013).
- [48] D. A. Huse, R. Nandkishore, and V. Oganesyan, *Phys. Rev. B* **90**, 174202 (2014).
- [49] V. Ros, M. Mueller, and A. Scardicchio, *Nuclear Physics B* **891**, 420 (2015).
- [50] J. Z. Imbrie, *Phys. Rev. Lett.* **117**, 027201 (2016).
- [51] T. B. Wahl, A. Pal, and S. H. Simon, *Phys. Rev. X* **7**, 021018 (2017).
- [52] M. Mierzejewski, M. Kozarzewski, and P. Prelovšek, *Phys. Rev. B* **97**, 064204 (2018).
- [53] S. J. Thomson and M. Schiró, *Phys. Rev. B* **97**, 060201 (2018).
- [54] D. J. Luitz and Y. B. Lev, [arXiv:1610.08993](https://arxiv.org/abs/1610.08993) (2016).
- [55] D. J. Luitz and Y. Bar Lev, *Phys. Rev. Lett.* **117**, 170404 (2016).
- [56] H. Tal-Ezer and R. Kosloff, *J. Chem. Phys.* **81**, 3967 (1984).
- [57] C. Leforestier, R. Bisseling, C. Cerjan, M. Feit, R. Friesner, A. Gulberg, A. Hammerich, G. Jolicard, W. Karleim, H.-D. Meyer, N. Lipkin, O. Roncero, and R. Kosloff, *J. Comput. Phys.* **94**, 59 (1991).
- [58] H. Fehske and R. Schneider, *Computational many-particle physics* (Springer, Germany, 2008).
- [59] J. Haegeman, J. I. Cirac, T. J. Osborne, I. Pižorn, H. Verschelde, and F. Verstraete, *Phys. Rev. Lett.* **107**, 070601 (2011).
- [60] T. Koffel, M. Lewenstein, and L. Tagliacozzo, *Phys. Rev. Lett.* **109**, 267203 (2012).
- [61] J. Haegeman, C. Lubich, I. Oseledets, B. Vandereycken, and F. Verstraete, *Phys. Rev. B* **94**, 165116 (2016).
- [62] S. Paeckel, T. Köhler, A. Swoboda, S. R. Manmana, U. Schollwöck, and C. Hubig, *Annals of Physics* **411**, 167998 (2019).
- [63] P. Naldesi, E. Ercolessi, and T. Roscilde, *SciPost Phys.* **1**, 010 (2016).
- [64] X. Wei, C. Cheng, G. Xianlong, and R. Mondaini, *Phys. Rev. B* **99**, 165137 (2019).
- [65] R. Yao and J. Zakrzewski, “Many-body localization in Bose-Hubbard model: evidence for the mobility edge,” [arXiv:2002.00381](https://arxiv.org/abs/2002.00381).
- [66] Q. Guo, C. Cheng, Z.-H. Sun, Z. Song, H. Li, Z. Wang, W. Ren, H. Dong, D. Zheng, Y.-R. Zhang, R. Mondaini, H. Fan, and H. Wang, “Observation of energy resolved many-body localization,” [arXiv:1912.02818](https://arxiv.org/abs/1912.02818).
- [67] T. C. Berkelbach and D. R. Reichman, *Phys. Rev. B* **81**, 224429 (2010).
- [68] K. Agarwal, S. Gopalakrishnan, M. Knap, M. Müller, and E. Demler, *Phys. Rev. Lett.* **114**, 160401 (2015).
- [69] S. Bera, H. Schomerus, F. Heidrich-Meisner, and J. H. Bardarson, *Phys. Rev. Lett.* **115**, 046603 (2015).
- [70] S. Bera, G. De Tomasi, F. Weiner, and F. Evers, *Phys. Rev. Lett.* **118**, 196801 (2017).
- [71] L. Herviou, S. Bera, and J. H. Bardarson, *Phys. Rev. B* **99**, 134205 (2019).
- [72] L. Colmenarez, P. A. McClarty, M. Haque, and D. J. Luitz, [arXiv:1906.10701](https://arxiv.org/abs/1906.10701).
- [73] P. Sierant and J. Zakrzewski, *Phys. Rev. B* **101**, 104201 (2020).
- [74] Y. Y. Atas, E. Bogomolny, O. Giraud, and G. Roux, *Phys. Rev. Lett.* **110**, 084101 (2013).
- [75] C. Lanczos, *Journal of Research of the National Bureau of Standards* **45** (1950).
- [76] S. R. White, *Phys. Rev. Lett.* **69**, 2863 (1992).
- [77] S. R. White, *Phys. Rev. B* **48**, 10345 (1993).
- [78] U. Schollwöck, *Rev. Mod. Phys.* **77**, 259 (2005).
- [79] U. Schollwöck, *Annals of Physics* **326**, 96 (2011).
- [80] R. Orús, *Annals of Physics* **349**, 117 (2014).
- [81] See supplementary material, which includes Refs. [82, 83], at [URL will be inserted by publisher] for additional results and brief description of computational methods performed via MPS.
- [82] T. Chanda, J. Zakrzewski, M. Lewenstein, and L. Tagliacozzo, *Phys. Rev. Lett.* **124**, 180602 (2020).
- [83] S. Goto and I. Danshita, *Phys. Rev. B* **99**, 054307 (2019).
- [84] D. J. Luitz, N. Laflorencie, and F. Alet, *Phys. Rev. B* **93**, 060201 (2016).
- [85] L. D’Alessio, Y. Kafri, A. Polkovnikov, and M. Rigol, *Advances in Physics* **65**, 239 (2016).

- [86] K. Agarwal, E. Altman, E. Demler, S. Gopalakrishnan, D. A. Huse, and M. Knap, *Annalen der Physik*, **529** (2016).
- [87] H. P. Lüschen, P. Bordia, S. Scherg, F. Alet, E. Altman, U. Schneider, and I. Bloch, *Phys. Rev. Lett.* **119**, 260401 (2017).
- [88] F. Weiner, F. Evers, and S. Bera, *Phys. Rev. B* **100**, 104204 (2019).
- [89] E. J. Torres-Herrera and L. F. Santos, *Phys. Rev. B* **92**, 014208 (2015).
- [90] E. J. Torres-Herrera and L. F. Santos, *Philosophical Transactions of the Royal Society A: Mathematical, Physical and Engineering Sciences* **375**, 20160434 (2017).
- [91] E. J. Torres-Herrera, A. M. García-García, and L. F. Santos, *Phys. Rev. B* **97**, 060303 (2018).
- [92] M. Schiulaz, E. J. Torres-Herrera, and L. F. Santos, *Phys. Rev. B* **99**, 174313 (2019).
- [93] P. Sierant and J. Zakrzewski, *New Journal of Physics* **20**, 043032 (2018).
- [94] P. Brighi, D. Abanin, and M. Serbyn, “Particle density mobility edge,” [arXiv:2005.02999](https://arxiv.org/abs/2005.02999).

Supplementary material to

“Many-body localization transition in large quantum spin chains: The mobility edge”

Titas Chanda,^{1,*} Piotr Sierant,^{1,†} and Jakub Zakrzewski^{1,2,‡}¹*Instytut Fizyki Teoretycznej, Uniwersytet Jagielloński, Łojasiewicza 11, 30-348 Kraków, Poland*²*Mark Kac Complex Systems Research Center, Uniwersytet Jagielloński, Kraków, Poland.*

(Dated: October 13, 2020)

Here, we first briefly describe the computational methods performed via matrix product state (MPS) in the main text. Then we also supplement the main text via additional results. Specifically, we discuss the dependence of the cut-off β_0 on the energy density and system-size.

A. Brief descriptions of the MPS calculations

For large system sizes, i.e., $L > 26$, we use matrix product states (MPS) ansatz [1, 2] to represent the quantum state of the disordered Heisenberg chain. The energies of the ground state (E_{\min}) and highest excited state (E_{\max}) are obtained using standard density matrix renormalization group method (DMRG) [1–5]. E_{\min} can simply be found from the ground-state search of H of Eq. (1) of the main text using DMRG, while that of $-H$ gives us $-E_{\max}$. In these calculations, we keep truncation error due to singular value decomposition (SVD) below 10^{-12} , i.e., we discard states corresponding to smallest singular values λ_n that satisfy $\frac{\sum_{n \in \text{discarded}} \lambda_n^2}{\sum_{n \in \text{all}} \lambda_n^2} < 10^{-12}$.

For time evolution large systems, i.e., $L > 26$, we employ MPS based time-dependent variational principle (TDVP) method [6–9]. Specifically, we use ‘hybrid’ scheme of TDVP [9–12] with step-size $\delta t = 0.1$, where two-site variant of TDVP is used initially to dynamically grow the bond dimension of the MPS, until the bond dimension in the bulk of the MPS is saturated to a pre-determined value χ_{\max} . One-site variant of TDVP is employed in the subsequent dynamics. In our calculations, we fix χ_{\max} to be 384, which gives reliable results up to $t = 500$. For a more detailed analysis of the convergence of TDVP in the disordered Heisenberg chain, see [11].

B. Imbalance vs density correlation function

The Néel state

$$|\psi_{\text{Néel}}\rangle = |\uparrow, \downarrow, \uparrow, \dots\rangle \quad (1)$$

was used in previous works [11, 13] to locate the transition to MBL phase. It is worth to mention that density wave states, analogous to the Néel state were used in experiment with ultra-cold fermions [14] that demonstrated signatures of MBL transition.

Imbalance $I(t)$ is the common name for the density correlation function (Eq. (2) of the main text) calculated

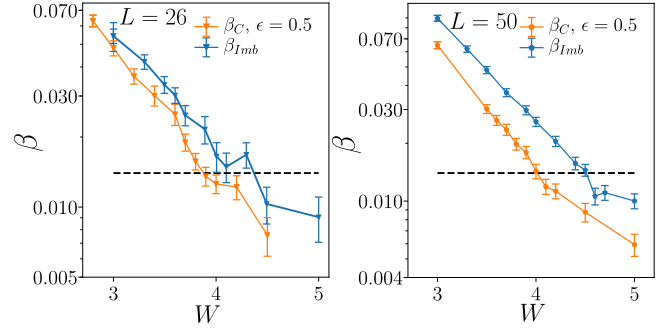


FIG. 1. The exponent β_C obtained in fitting the density correlation function $C(t)$ with an algebraic decay $a_0 t^{-\beta}$ in interval $t \in [100, 500]$ for rescaled energy $\epsilon = 0.5$ of the initial state together with exponent β_{Imb} obtained from the fitting of $I(t)$ for Néel state in the same time interval. Error bars dictate 1σ errors in β obtained from statistical resampling procedure. Left: system size $L = 26$, Right: system size $L = 50$.

for the Néel state. The imbalance behaves similarly to the density correlation function: initially it decreases and oscillates, subsequently it decays algebraically in time. Fig. 1 shows comparison of exponents β_C and β_{Imb} that govern the power-law decay of $C(t)$ correlation function for rescaled energy of initial state $\epsilon = 0.5$ (which is the rescaled energy corresponding to the Néel state), and power-law decay of imbalance of Néel state. The exponents β_{Imb} are consistently bigger than β_C . This fact may be traced back to the number of states coupled by the Hamiltonian (Eq. (1) of the main text) to state $|\psi_{\text{Néel}}\rangle$ which is higher than the average number of states coupled to a typical Fock state with $\epsilon = 0.5$. The absence of aligned spins on neighboring sites makes the thermalization process more efficient for Néel state. The inequality $\beta_C < \beta_{Imb}$ justifies the cut-off beta value $\beta_0^{Imb} = 0.02$ for decay of imbalance in Néel state assumed in [11].

C. Energy and system size dependence of the cut-off value β_0

The cut-off value $\beta_0 = 0.014$ assumed in the main text, was obtained from comparison of exact diagonalization results for systems of size $L \leq 22$ with the exponent β governing the power-law decay of density corre-

* titas.chanda@uj.edu.pl

† piotr.sierant@uj.edu.pl

‡ jakub.zakrzewski@uj.edu.pl

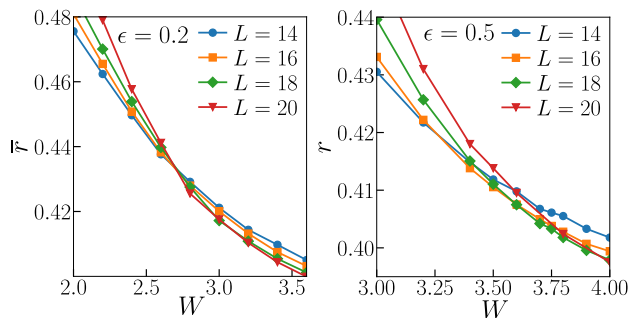


FIG. 2. The average gap ratio \bar{r} for random field Heisenberg spin chain for rescaled energies $\epsilon = 0.2$ (left panel) and $\epsilon = 0.5$ (right panel) for different system-sizes $L \leq 20$.

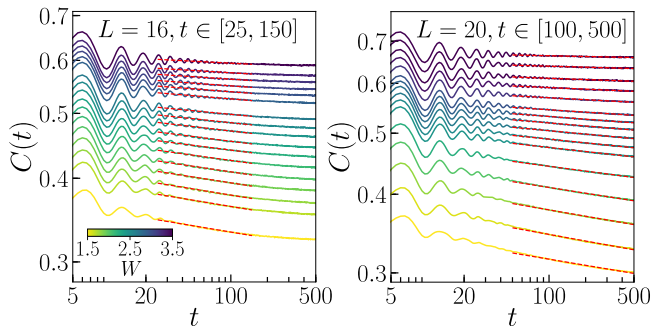


FIG. 3. Density correlation function $C(t)$ for system sizes $L = 16, 20$ – left and right panel, respectively; rescaled energy of the initial state $\epsilon = 0.2$, disorder strength $W = 1.5, \dots, 3.5$ (color coded). Data are averaged over more than 5000 disorder realizations. Power-law fits $C(t) \propto t^{-\beta}$ in time intervals denoted on respective panels are denoted by the dashed lines.

lation function $C(t)$ for system size $L = 20$. This procedure leads, however, to questions about dependence of the cut-off β_0 on the rescaled energy ϵ and on the system size L . To answer the question about energy dependence, we consider two representative values of the rescaled energy $\epsilon = 0.2, 0.5$. The system size dependence of β_0 is probed by studying Heisenberg spin chains of length $L = 14, 16, 18, 20$.

Using eigenvalues E_i obtained in the exact diagonalization, we calculate the gap ratios $r_i = \min\{\frac{s_{i+1}}{s_i}, \frac{s_i}{s_{i+1}}\}$, where $s_i = E_{i+1} - E_i$, and average it over small fraction of system spectrum around the rescaled energy ϵ and over more than 2000 disorder realizations obtaining an average gap ratio \bar{r} , shown in Fig. 2. The average gap ratio changes between $\bar{r} \approx 0.53$ in ergodic phase of systems with time reversal invariance and $\bar{r} \approx 0.39$ in MBL phase [15]. In the calculations of the average gap ratio \bar{r} we use periodic boundary conditions to probe the bulk properties of the system that are also reflected by the density correlation function $C(t)$ (for which we disregard the two sites at the boundary of the system).

As an approximation for critical disorder strength at given system size L , we use, following [16], disorder

strength $W_C(L)$ at which the curves $\bar{r}(W)$ for L and $L + 2$ cross. For the rescaled energy $\epsilon = 0.2$ we obtain $W_C^{\epsilon=0.2}(L) \approx 2.7$ for all the system sizes considered. Drift of the crossing points is much more pronounced for the rescaled energy $\epsilon = 0.5$ for which we obtain $W_C^{\epsilon=0.5}(L = 14) \approx 3.3$ which increases with system size L up to $W_C^{\epsilon=0.5}(L = 18) \approx 3.85$.

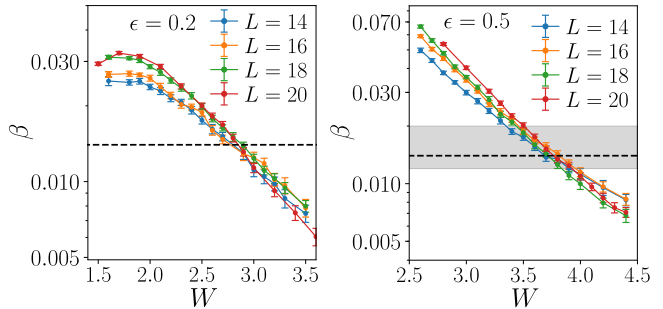


FIG. 4. The exponent β , obtained in fitting the density correlation function $C(t)$ with an algebraic decay $a_0 t^{-\beta}$ is plotted as function of disorder strength W for the rescaled energy $\epsilon = 0.2$ (left panel) and $\epsilon = 0.5$ (right panel). The error bars represent the 1σ errors of the fitting obtained from statistical resampling of disorder realizations. The dashed line shows the cut-off exponent $\beta_0 = 0.014$.

The obtained approximations of critical disorder strength $W_C^{\epsilon=0.5}(L)$ can now be used to find the corresponding values of cut-off β_0 at system size L . To that end, we calculate density correlations functions (examples shown in Fig. 3) for $14 \leq L \leq 20$. Exponents β are obtained by power-law fits to $C(t)$. At small system sizes, $C(t)$ tend to saturate at times of the order of few hundred (in units of J^{-1}) that roughly correspond to inverse level spacing at the rescaled energy ϵ . Thus, we vary the interval in which fitting is performed with system size: $t \in [20, 100]$ for $L = 14$; $t \in [25, 150]$ for $L = 16$; $t \in [50, 300]$ for $L = 18$ and $t \in [100, 500]$ for $L = 20$. The resulting values of β are shown in Fig. 4. For $\epsilon = 0.2$, we observe that $W_C^{\epsilon=0.2} \approx 2.7$ is consistent with the cut-off $\beta_0 = 0.014(2)$, confirming that the cut-off $\beta_0 = 0.014$ can be used globally, for all considered values of the rescaled energy. For $\epsilon = 0.5$, the drift of the crossing point $W_C^{\epsilon=0.5}(L = 14) \approx 3.3$ to $W_C^{\epsilon=0.5}(L = 18) \approx 3.85$ corresponds to change in value of the β_0 between 0.02 and 0.012 – as denoted by the shaded area in Fig. 4. This decreasing trend of β_0 with system size L at $\epsilon = 0.5$ might suggest that the cut-off value decreases with system size. Within the current approach we are unable to conclude whether β_0 decreasing with system size is a better hypothesis than the constant value of β_0 . This illustrates the difficulties inherent to studying MBL transition in thermodynamic limit, described, e.g. in [17]. Nevertheless, as Fig. 7 of the main text shows, changes of the cut-off β_0 in range from 0.01 to 0.02 do not affect our conclusions about the existence or the shape of the many-body mobility edge in the system.

-
- [1] R. Orús, *Annals of Physics* **349**, 117 (2014).
- [2] U. Schollwöck, *Annals of Physics* **326**, 96 (2011).
- [3] S. R. White, *Phys. Rev. Lett.* **69**, 2863 (1992).
- [4] S. R. White, *Phys. Rev. B* **48**, 10345 (1993).
- [5] U. Schollwöck, *Rev. Mod. Phys.* **77**, 259 (2005).
- [6] J. Haegeman, J. I. Cirac, T. J. Osborne, I. Pizorn, H. Verschelde, and F. Verstraete, *Phys. Rev. Lett.* **107**, 070601 (2011).
- [7] T. Koffel, M. Lewenstein, and L. Tagliacozzo, *Phys. Rev. Lett.* **109**, 267203 (2012).
- [8] J. Haegeman, C. Lubich, I. Oseledets, B. Vandereycken, and F. Verstraete, *Phys. Rev. B* **94**, 165116 (2016).
- [9] S. Paeckel, T. Köhler, A. Swoboda, S. R. Manmana, U. Schollwöck, and C. Hubig, *Annals of Physics* **411**, 167998 (2019).
- [10] S. Goto and I. Danshita, *Phys. Rev. B* **99**, 054307 (2019).
- [11] T. Chanda, P. Sierant, and J. Zakrzewski, *Phys. Rev. B* **101**, 035148 (2020).
- [12] T. Chanda, J. Zakrzewski, M. Lewenstein, and L. Tagliacozzo, *Phys. Rev. Lett.* **124**, 180602 (2020).
- [13] E. V. H. Doggen, F. Schindler, K. S. Tikhonov, A. D. Mirlin, T. Neupert, D. G. Polyakov, and I. V. Gornyi, *Phys. Rev. B* **98**, 174202 (2018).
- [14] M. Schreiber, S. S. Hodgman, P. Bordia, H. P. Lüschen, M. H. Fischer, R. Vosk, E. Altman, U. Schneider, and I. Bloch, *Science* **349**, 842 (2015).
- [15] V. Oganesyan and D. A. Huse, *Phys. Rev. B* **75**, 155111 (2007).
- [16] P. Sierant, M. Lewenstein, and J. Zakrzewski, “Polynomially filtered exact diagonalization approach to many-body localization,” [arXiv:2005.09534](https://arxiv.org/abs/2005.09534).
- [17] R. K. Panda, A. Scardicchio, M. Schulz, S. R. Taylor, and M. Žnidarič, *EPL (Europhysics Letters)* **128**, 67003 (2020).